Pediatr Radiol (2009) 39 (Suppl 2):S191–S195
DOI 10.1007/s00247-008-1118-0

REVIEW

What is the optimal imaging for vascular rings and slings?

Lorna P. Browne

Keywords Vascular ring · Pulmonary sling · MRI · CTA · Pediatrics

Embryology

The schematic diagrams of the 'hypothetical double aortic arch' introduced by Stewart et al. have been widely used to conceptualize the embryological origin of different anomalies of the aortic arch [1]. Briefly, in embryonic vascular development, ventral and dorsal aortae are connected by six pairs of aortic/branchial arches. In normal development, the first, second, and fifth arches and a portion of the right fourth arch regress; this results in 'the usual' left aortic arch. The residual third arch forms the common carotid arteries bilaterally. The residual segments of the right fourth arch, together with a vessel called the seventh intersegmental artery, form the right subclavian artery. The sixth arch forms the ductus arteriosus and the proximal portions of the right and left pulmonary arteries (RPA and LPA) (Fig. 1). The intraparenchymal portions of the pulmonary arteries are derived from their respective lung buds and join the proximal RPA and LPA respectively. Inappropriate persistence or development of segments of the primitive vascular system account for most of the congenital vascular rings and slings.

Dr. Browne has indicated that she has no relevant financial relationships or potential conflicts or interest related to the material presented.

L. P. Browne (✉)
Edward B Singleton Department of Diagnostic Imaging,
Texas Children's Hospital,
MC-2251, 6621 Fannin Street,
Houston, TX 77030, USA
e-mail: lxbrowne@texaschildrens.org

Anatomy and description

The most commonly encountered symptomatic vascular ring is a double aortic arch. Usually both arches are patent (Fig. 2). The right arch tends to be higher and dominant in the majority of cases with the left arch hypoplastic or atretic (approximately 70% of cases). In the remainder of cases, either both arches are the same size or rarely, the right arch is atretic. The second most commonly encountered vascular ring is the right sided aortic arch with aberrant left subclavian artery and left sided ligamentum arteriosus (Fig. 3). Normally, the ligamentum arteriosus is on the same side as the aortic arch. Occasionally it develops on the contralateral side to the arch completing a vascular ring. The ring encountered in a right sided aortic arch with aberrant left subclavian artery and left sided ligamentum arteriosus tends to be looser then those encountered in double arches, and therefore this is frequently identified as an incidental anomaly. Other less commonly encountered vascular rings include right aortic arch with mirror image branching and left-sided ligamentum arteriosus, left aortic arch with aberrant right subclavian artery and right-sided ligamentum arteriosum, and circumflex aorta (where the descending aorta crosses behind the esophagous and descends on the opposite side of the arch). Circumflex aortas can occur with both left and right sided aortic arches and are also associated with a ligamentum arteriosus located on the contralateral side to the arch which completes the ring (Fig. 4).

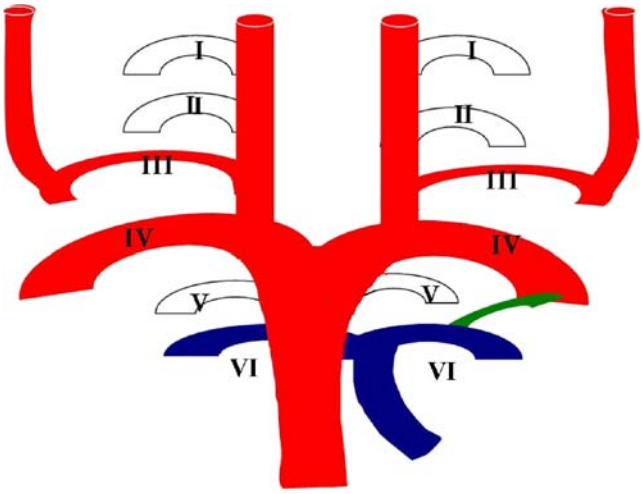

Fig. 1 Embryological development of the aortic arches

The identification of atretic structures completing a vascular ring, such as a ligmentum arteriosus or the atretic limb of a double aortic arch, is fundamental to the vascular ring evaluation. The presence of these atretic structures can be recognized by the presence of one of the 3 'D's on the opposite side to the arch (dimple, diverticulum or descending aorta). Kommerell's original description of a diverticulum was originally described in the setting of a left sided aortic arch with an aberrant right subclavian artery and a right sided ligamentum arteriosum, which is an extremely rare type of vascular ring. However the term 'diverticulum of Kommerell' is now more commonly attributed to a right sided aortic arch with aberrant left subclavian artery. The diverticulum occurs at the site of the aberrant subclavian artery and represents the aortic attachment of a ligamentum arteriosus. It can be recognized by the change in caliber which occurs as the broad-based diverticulum ends and the aberrant subclavian artery begins. Additional imaging features such as the four-vessel sign and the acute angle of origin of the proximal left subclavian artery origin can assist in distinguishing a double aortic arch with an atretic distal left limb from a right sided arch with mirror image branching [2, 3]. The four-vessel sign represents the symmetry of the brachio-cephalic vessels at a level just cephalad to the aortic arch. The distortion of the proximal portion of the subclavian artery is due to tethering to the atretic remnant of a left arch.

In the pulmonary sling complex, the anomalous left pulmonary artery arises from an elongated right pulmonary artery, turns dorsally encircling the right main bronchus, passes to the left between the trachea and esophagus, and enters the hilum of the left lung. Both the right main bronchus and the trachea are constricted. The left and right main bronchi have a horizontal course resulting in a 'T-shaped' trachea.

Associated anomalies

Pulmonary slings are associated with complete 'O-shaped' cartilaginous tracheal rings in approximately 40–50% of cases. The segment with complete rings is usually narrowed. The length of the tracheal stenosis is frequently extensive, making reconstruction difficult. The decision to repair the trachea is based on the presence of clinical symptoms indicating moderate to severe stenosis and the degree of tracheal narrowing identified on preoperative imaging [4]. Other airway anomalies seen with pulmonary slings include a bridging bronchus, which represents an anomalous bronchus to the right originating from the left main bronchus and tracheal bronchus, where the right upper lobe bronchus arises as an independent branch from the trachea.

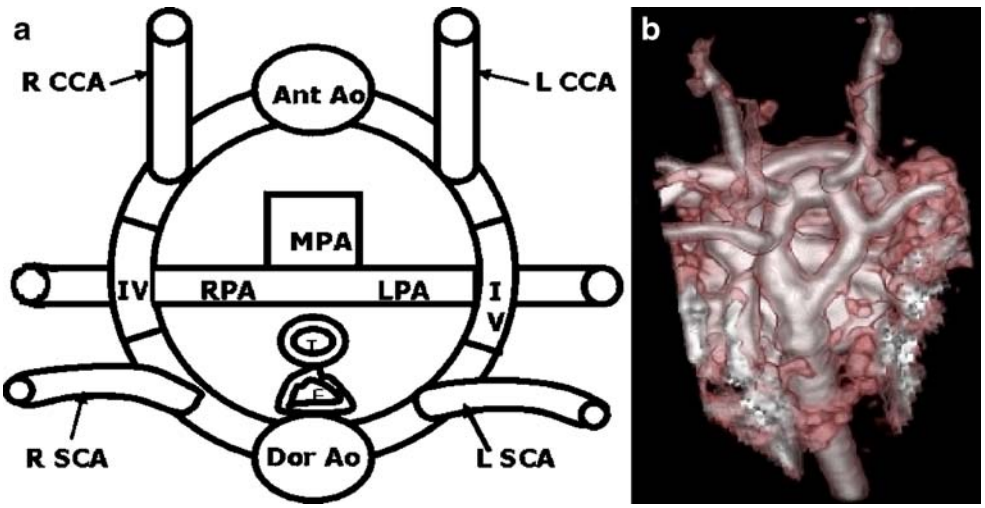

Fig. 2 Double aortic arch. **a** Schematic diagram of Double Aortic Arch. **b** 3 dimensional volume-rendered image from contrast-enhanced MR angiogram demonstrating patency of both arches

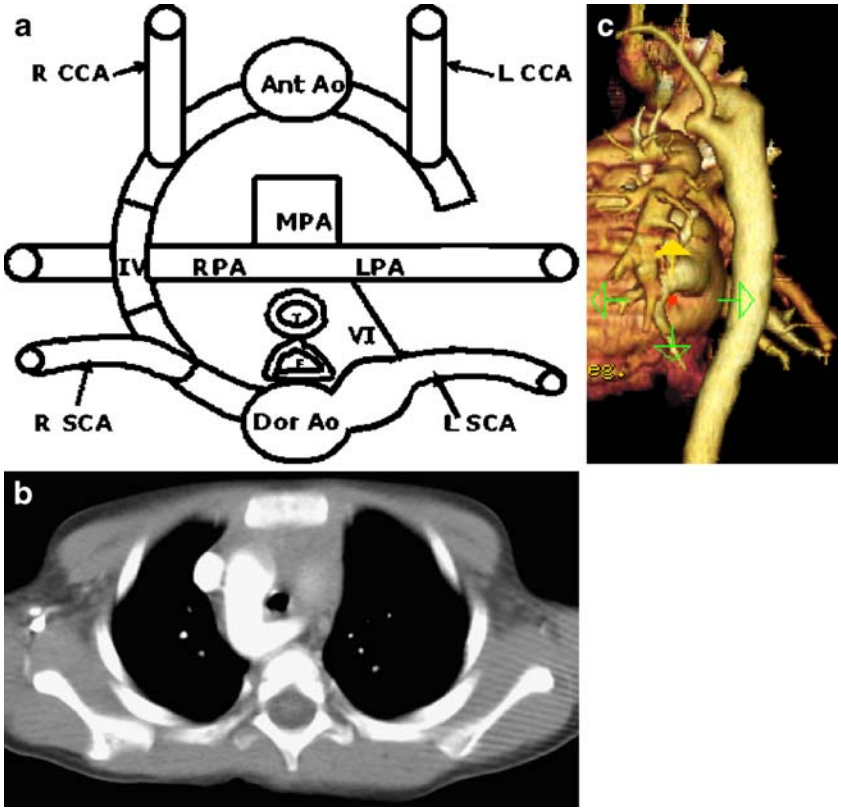

Fig. 3 Right Aortic Arch with aberrant Left Subclavian Artery and Left sided Ligamentum Arteriosus. **a** Schematic diagram of Right Aortic Arch with aberrant Left Subclavian Artery and Left sided Ligamentum Arteriosus. **b** Axial CTA of aberrant retroesophageal left SCA. **c** Posterior view of 3 dimensional Volume-Rendered Image from contrast-enhanced CT angiogram demonstrating broad based diverticulum at origin of left SCA indicating the presence of a left sided ligamentum arteriosus

Vascular rings can also be associated with abnormal development of the tracheo-bronchial tree resulting in tracheomalacia and tracheal stenosis.

Congenital heart disease and anomalous systemic or pulmonary venous drainage should be a consideration in all patients being evaluated for a vascular ring. Right sided aortic arch (usually with mirror image branching) is associated with associated congenital heart disease in approximately 50% of cases. These include tetralogy of Fallot, truncus arteriosus, double outlet right ventricle, pulmonary stenosis with a ventricular septal defect (VSD) and tricuspid atresia.

Renal anomalies such as renal agenesis, cross-fused ectopia and horse-shoe kidneys can also be an unsuspected finding in patients undergoing evaluation for a vascular ring.

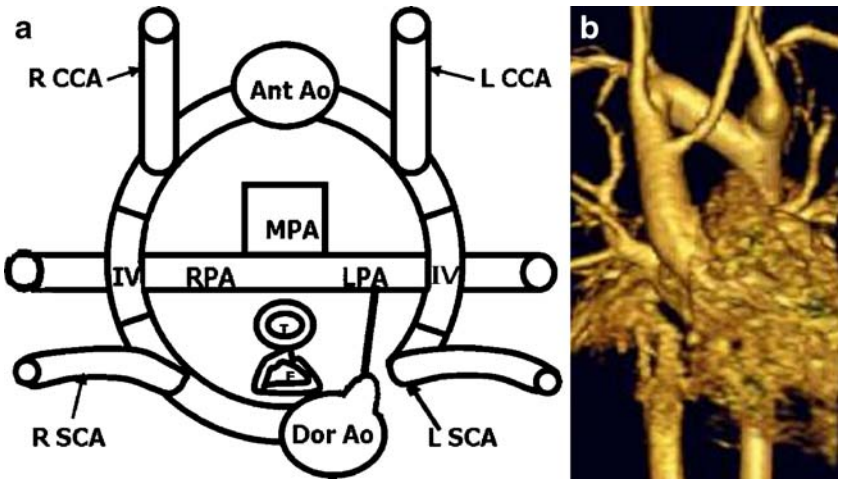

Fig. 4 Circumflex aorta. **a** Schematic diagram of Circumflex Aorta with right sided aortic arch and left sided descending aorta. **b** 3 dimensional Volume-Rendered Image from contrast-enhanced MR angiogram demonstrating right sided aortic arch with a left sided descending aorta and left sided diverticulum

Imaging evaluation

Chest X-ray The imaging evaluation of a vascular ring typically begins with the conventional chest X-ray. Both frontal and lateral views are necessary for appreciation of a vascular ring. The mediastinum should be carefully evaluated for the presence of a right sided or double aortic arch and narrowing of the trachea at the site of the aortic knuckle. On the lateral view, anterior bowing of the trachea and an increase in the retro-tracheal soft tissues may also be appreciated. At least one of these findings is reported to be visible in greater than 95% of cases, and at least two findings in greater than 90% of cases [5].

The chest X-ray findings in pulmonary sling include unilateral aeration, tracheal narrowing and an unusual horizontal course to the left main bronchus [6].

Upper GI examination Barium esophagography has historically been a reliable study for the diagnosis of a vascular ring [7]. The location of the aortic arch in relation to the trachea can be determined. A posterior indentation suggests an aberrant subclavian artery and an aberrant left subclavian artery will usually produce an oblique indentation angled toward the left shoulder. Bilateral persistent indentations on the esophagus on the anteroposterior view suggest a double arch. The diagnosis of a vascular ring can usually be established although determining the specific type of ring with chest radiographs and esophagograms alone is usually not possible.

Anterior pulsatile indentation of the esophagus outlined on balrium swallow is virtually pathognomonic for pulmonary artery sling, but the examination is contraindicated in critically ill neonates, especially if ventilator dependent [4].

Echocardiogram and conventional angiogram Traditionally an upper GI examination followed by echocardiogram (ECHO) and conventional aortogram were used to establish the diagnosis. ECHO has sensitivities which vary between 30–100% depending on the study [8, 9]. ECHO has the advantage of a comprehensive assessment of intracardiac anatomy and function; however it is limited by acoustic windows, high interobserver variability and lack of depiction of airway/esophageal involvement. Conventional angiography is invasive, and is limited by high radiation dose and need for iodinated contrast material. When these methods are used additional airway investigation with bronchoscopy is required [10].

CT angiography and MR angiography Non-invasive angiography with MDCT and MR has widely replaced other techniques. Both of these modalities have sensitivities approaching 100% [11, 12]. However there is on-going debate about whether CTA or MRA should be the preferred investigation.

MDCT has the advantages of easy availability and very short scanning times. Contrast-enhanced MDCT allows the precise timing necessary for accurate extra-cardiac arterial and venous vascular imaging. The drawbacks of CT include ionizing radiation and need for iodinated contrast material. Adjustment of specific technical factors has been shown to minimize the radiation dose in children undergoing CT. Such adjustment includes setting the lowest diagnostic tube current according to patient weight (range, 40–140 mA for chest CT). In addition, doubling the pitch reduces radiation dose by half. A practical standard pitch for single-detector row helical CT in children is 1.5:1.

MDCT enables precise evaluation of the airway in patients with suspected tracheobronchomalacia. In cooperative children, CT images can be acquired during volitional breath-holding at full inspiration and end expiration to depict maximal changes in airway caliber. In uncooperative children, CT images can be acquired at desired degrees of airway distention by the controlled-ventilation technique used in sedated patients without intubation. With this technique, several sequential inspirations are augmented by face-mask ventilation to induce hypocarbia and the Hering-Breuer reflex, which results in brief apneic periods during which images can be acquired. In uncooperative children in whom the controlled-ventilation technique is not feasible or available, cine CT can be used to rapidly acquire images of the airway throughout the respiratory cycle during free breathing. After the site of suspected airway stenosis or malacia is located, CT images are rapidly and sequentially acquired at the same axial level by setting the table increment to zero. With the sub-half-second gantry rotation times and partial scan reconstruction; cine CT technique can provide multiple images of the airway during inspiration and expiration, even in tachypneic patients. Contemporary MDCT scanners can generate the high-quality volumetric data sets required for multiplanar and three-dimensional (3D) image reconstruction, including volume-rendered imaging and virtual bronchoscopy. One substantial advantage of CT over direct bronchoscopy is its ability to show synchronous lesions distal to obstructive lesions not passable by the bronchoscope. This includes the depiction of a bridging bronchus in patients with pulmonary sling, since direct bronchoscopic visualisation may not be possible due to the presence of significant proximal stenoses; and even when visualized it can be challenging to differentiate the bifurcation from the pseudocarina [13]. CT can also depict the effects (eg, collapse, air trapping, mucus plugging) of a proximal obstructive lesion on the distal airways and lungs.

The direct multiplanar imaging capability of MR imaging allows precise depiction of vascular anatomy and enables comprehensive evaluation of associated intracardiac defects at a single sitting. MRI avoids the need for ionizing radiation and iodinated contrast material.

Previously multiple acquisitions resulting in long examinations made this investigation unsuitable for the sick or young without sedation. Now rapid image acquisition sequences such as single-shot T1 weighted echo-planar imaging and 2-D/3-D steady state free precession sequences enable more rapid multiplanar evaluation with reduced need for sedation. Contrast-enhanced MR angiography using a time-resolved technique in the pediatric patient enables rapid data collection while maintaining adequate spatial resolution [14]. Faster acquisition is enabled by parallel imaging techniques and undersampling of K-space. The disadvantage of parallel imaging is a decreased signal-to-noise ratio (S/N), however this is counteracted by increased vascular S/N that intravenous gadolinium contrast agents provide, even with the variable injection rates and small volumes used in infants and children.

Static evaluation of the pediatric airway is performed using high resolution T1 weighted sequence with minimal gap. The trachea can also be dynamically evaluated for tracheomalacia using an ultrafast gradient echo pulse sequence with data acquisition after an initial 180 preparation pulse. Images are obtained during quiet respiration and are reviewed in a cine format, using the position of the anterior chest wall to assess the phase of respiration. This method has demonstrated excellent correlation when compared with bronchoscopy for the assessment of tracheal collapsibility [15, 16].

However despite the high accuracy that both CT and MRI display in evaluating the associated findings in the tracheo-bronchial tree, in clinical practice some patients still undergo direct visualization with bronchoscopy prior to surgical repair.

Conclusion

Ultimately the decision to image with CT versus MR should take into consideration institutional equipment, scheduling, availability as well as the patient's ability to cooperate. Avoidance of unnecessary radiation in the pediatric population favors the use of MRI, while the presence of a pulmonary sling with its multiple co-existent tracheo-bronchial abnormalities and distal effects on lung parenchyma are better evaluated with MDCT given the variety of techniques that allow for precise pre-surgical airway evaluation.

References

1. Stewart JR, Kincaid OW, Edwards JE (1964) An atlas of vascular rings and related malformations of the aortic system. Charles C Thomas, Springfield
2. Schlesinger AE, Krishnamurthy R, Sena LM et al (2005) Incomplete double aortic arch with atresia of the distal left arch: distinctive imaging appearance. AJR Am J Roentgenol 184:1634–1639
3. Holmes KW, Bluemke DA, Vricella LA et al (2006) Magnetic resonance imaging of a distorted left subclavian artery course: an important clue to an unusual type of double aortic arch. Pediatr Cardiol 27:316–320
4. Fiore AC, Brown JW, Weber TR et al (2005) Surgical treatment of pulmonary artery sling and tracheal stenosis. Ann Thorac Surg Jan 79:38–46
5. Pickhardt PJ, Siegel MJ, Gutierrez FR (1997) Vascular rings in symptomatic children: frequency of chest radiographic findings. Radiology 203:423–426
6. Berdon WE, Baker DH, Wung JT et al (1984) Complete cartilage-ring tracheal stenosis associated with anomalous left pulmonary artery: the ring-sling complex. Radiology 152:57–64
7. Neuhauser EBD (1946) The Roentgen diagnosis of double aortic arch and other anomalies of the great vessels. AJR Am J Roentgenol 56:1–12
8. van Son JA, Julsrud PR, Hagler DJ et al (1994) Ann Thorac Surg 57:604–610
9. Lillehei CW, Colan S (1992) Echocardiography in the preoperative evaluation of vascular rings. Pediatr Surg 27:1118–1120
10. Task Force of the European Society of Cardiology, in collaboration with the Association of European Paediatric Cardiologists (1998) The clinical role of magnetic resonance in cardiovascular disease. Eur Heart J 19:19–39
11. Turner A, Gavel G, Coutts J (2005) Vascular rings—presentation, investigation and outcome. Eur J Pediatr 164:266–270
12. Malik TH, Bruce IA, Kaushik V et al (2006) The role of magnetic resonance imaging in the assessment of suspected extrinsic tracheobronchial compression due to vascular anomalies. Arch Dis Child 91:52–55
13. Baden W, Schaefer J, Kumpf M et al (2008) Comparison of imaging techniques in the diagnosis of bridging bronchus. Eur Respir J 31:1125–1131
14. Chung T, Krishnamurthy R (2005) Contrast-enhanced MR angiography in infants and children. Magn Reson Imaging Clin N Am 13:161–170
15. Faust RA, Rimell FL, Remley KB (2002) Cine magnetic resonance imaging for evaluation of focal tracheomalacia innominate artery compression syndrome. Int J Pediatr Otorhinolaryngol. 65:27–33
16. Faust RA, Remley KB, Rimell FL (2001) Real-time, cine magnetic resonance imaging for evaluation of the pediatric airway. Laryngoscope 111:2187–2190